Multiband theory of Bloch-electron dynamics in a homogeneous electric field

Jun He
Department of Electrical and Computer Engineering, North Carolina State University, North Carolina 27695-7911

Gerald J. Iafrate
U.S. Army Research Office, Research Triangle Park, North Carolina 27709-2211
(Received 24 May 1993; revised manuscript received 20 April 1994)

A multiband theory of Bloch electron dynamics in a uniform electric field of arbitrary strength is presented. In this formalism, the electric field is described through the use of the vector potential. Multiband coupling is treated through the use of the Wigner-Weisskopf approximation, thus allowing for a Bloch-electron transition out of the initial band due to the power absorbed by the electric field; also, the approximation insures conservation of total transition probability over the complete set of excited bands. The choice of the vector-potential gauge leads to a natural set of extended time-dependent basis functions for describing Bloch-electron dynamics in a homogeneous electric field; an associated basis set of localized, electric-field-dependent Wannier and related envelope functions are utilized in the analysis to demonstrate the inherent localization manifest in Bloch dynamics in the presence of relatively strong electric fields. From the theory, a generalized Zener tunneling time is derived in terms of the applied uniform electric field and the relevant band parameters; specific results are derived from the general theory using a nearest-neighbor tight-binding, multiband model, and are shown to have identical parametric dependence on electric field, but different, more realistic dependence on the appropriate band-structure parameters than those of the well-known Kane and effective-mass two-band model. Further, the analysis shows an electric-field-enhanced broadening of the excited-state probability amplitudes, thus resulting in spatial lattice delocalization and the onset of smearing of discrete, Stark-ladder, and band-to-band transitions due to the presence of the electric field.

I. INTRODUCTION

Bloch-electron dynamics in a homogeneous electric field has been a subject of great interest dating back to the earliest applications of quantum mechanics to solid-state physics.[1-3] Even more recently, as modern fabrication technologies continue to drive the study of solid-state transport into the nanometer domain, many interesting questions have emerged concerning the solid-state dynamics and quantum transport of carriers in "band-engineered" superlattices and tailored periodic solids.

Foremost among current questions are the age-old, controversial issues concerning the existence of Bloch oscillations and electric-field-induced Stark-ladder energy levels. Recent optical experiments, on excitonic emission from double wells[4] and four-wave mixing from superlattices,[5,6] and optical-absorption studies clearly indicated oscillatory electron dynamics and the manifestation of concomitant Stark-ladder transitions when optical probing is invoked; on the other hand, Bloch oscillations have been elusive in transport experiments, save for several reports of negative differential resistance observations[7-10] ascribed to Bloch oscillatory phase breaking due to the onset of scattering.

No doubt, there is still work to be done in developing the ultimate fundamental resolution of issues concerning the experimental manifestations of Bloch oscillations and the apparent differences observed in transport versus optical-absorption experiments. Resolution of these and other profound issues of quantum transport and optical absorption in the solid state require a fundamental, first-principles description of Bloch-electron dynamics in the presence of homogeneous electric fields of arbitrary strength. Therefore, the purpose of this paper is to extend the zero-order theory of Bloch-electron dynamics in homogeneous electric fields to include implicitly the effects of real band structure in a multiband analysis; as such, the theory derives the dependence of the Zener tunneling time on real band-structure parameters and quantum-mechanical initial conditions.

In this paper, a multiband theory of Bloch-electron dynamics in homogeneous electric fields of arbitrary strength is presented. In this formalism, the electric field is described through the use of the vector potential; in this regard, this work is a major extension of the methodology previously developed by one of the authors (G.J.I.) and co-workers[1-3] to describe solid-state dynamics and quantum transport for Bloch electrons in an applied homogeneous electric field of arbitrary strength and time dependence, including weak scattering from randomly distributed impurities and phonons,[1] and a spatially localized, inhomogeneous electric field.[3] The present paper extends the transition rate theory well beyond the short-time, time-dependent perturbation theory treatment of Krieger and Iafrate[1] to a long-time, multiband analysis. The multiband coupling is treated in the Wigner-Weisskopf (WW) (Ref. 11) approximation, a classic approach for describing the time decay from an occupied quasistationary state; the WW approximation allows

for the analysis of the long-time, time-dependent tunneling characteristics of an electron transition out of an initially occupied band due to the power absorbed by the electric field, while preserving the conservation of total transition probability over the complete set of excited bands.

The choice of the vector potential gauge leads to a natural set of basis functions for describing Bloch-electron dynamics in a homogeneous electric field. As shown in Sec. II, a basis set of localized, electric-field-dependent Wannier functions and associated envelope equations are utilized to accommodate the inherent localization manifest in Bloch dynamics due to a relatively strong electric field. Further, in Sec. III, the Wannier envelope equations and functions are analyzed for the case of the one-band approximation.

In Sec. IV, a multiband analysis is obtained by solving the coupled set of envelope equations through the use of the WW approximation. From the formalism, a generalized Zener tunneling time is derived for the initial ground state in terms of the applied electric field and pertinent band parameters; specific tunneling results from the application of the nearest-neighbor tight-binding multiband model are also derived, and are shown to have a similar parametric dependence on electric field, but with different, more realistic band-structure parameter dependence than the familiar Kane two-band model.[12] Further, the analysis also reveals that the envelope functions of the excited bands become delocalized in lattice space, and undergo an electric-field-enhanced broadening in probability amplitude which eventually results in the smearing of the discrete, Stark-ladder, and band-to-band transitions.

II. DYNAMICAL BLOCH AND WANNIER REPRESENTATION

Building on previous methodology,[3] use is made of the instantaneous eigenstates of the Hamiltonian describing a Bloch electron in an electric field:

$$H=\frac{1}{2m}\left[\mathbf{P}-\frac{e}{c}\mathbf{A}_0(t)\right]^2+V_c(\mathbf{x}) , \tag{1}$$

where $V_c(\mathbf{x})$ is crystal potential, $\mathbf{A}_0=-c\mathbf{E}_0 t$ is the vector potential for the time-independent homogeneous electric field $\mathbf{E}_0$, turned on at initial time $t=0$. It is noted that the basis states are

$$\phi_{n\mathbf{K}}(x,t)=\frac{e^{i\mathbf{K}\cdot\mathbf{x}}}{\Omega^{1/2}}U_{n\mathbf{k}(t)}(\mathbf{x}) , \tag{2}$$

where $U_{n\mathbf{k}(t)}$ is the periodic part of the usual Bloch function with band index "n" and wave vector $\mathbf{k}(t)$, given by

$$\mathbf{k}(t)=\mathbf{K}+\frac{e\mathbf{E}_0}{\hbar}t , \tag{3}$$

where $\mathbf{K}$ is a constant determined by the periodic boundary conditions in a box of volume Ω.

In the Wannier representation, the instantaneous Bloch functions of Eq. (2) are equivalently expressed as

$$\phi_{n\mathbf{K}}(\mathbf{x},t)=\frac{1}{\sqrt{N}}\sum_l e^{i\mathbf{K}\cdot l}W_n(\mathbf{x}-l,t) , \tag{4}$$

where N is the number of lattice sites, $W_n(\mathbf{x}-\mathbf{l},t)$ are the instantaneous Wannier functions for a Bloch electron in a spatially homogeneous electric field. Equation (4) can be inverted, so that

$$W_n(\mathbf{x}-l,t)=\frac{1}{\sqrt{N}}\sum_{\mathbf{K}} e^{-i\mathbf{K}\cdot l}\phi_{n\mathbf{K}}(\mathbf{x},t) . \tag{5}$$

As shown in Ref. 3, both $\phi_{n\mathbf{K}}$ of Eq. (4) and $W_n(\mathbf{x}-l,t)$ of Eq. (5) are complete sets of functions which can serve as a basis for the general solution to the Schrödinger equation in this problem. Therefore, the solution to the time-dependent Schrödinger equation for the Hamiltonian of Eq. (1) can be expanded as

$$\Psi=\sum_n\sum_l f_n(l,t)W_n(\mathbf{x}-l,t) , \tag{6}$$

where $f_n(l,t)$ is the envelope function in the Wannier representation. It was shown in previous work[3] that $f_n(l,t)$ obeys the equation

$$i\hbar\frac{\partial f_n(l,t)}{\partial t}=\sum_{n'}\sum_{l'}[\varepsilon_{n'}(l'-l,t)\delta_{nn'} -e\mathbf{E}_0\cdot\boldsymbol{\Delta}_{nn'}(l'-l,t)]f_{n'}(l',t) . \tag{7}$$

In Eq. (7), $\varepsilon_n(l-l',t)$ and $\boldsymbol{\Delta}_{nn'}(l-l',t)$ are given by

$$\varepsilon_n(l-l',t)=\frac{1}{N}\sum_{\mathbf{K}} e^{-i\mathbf{K}\cdot(l-l')}\epsilon_n\left[\mathbf{K}-\frac{e}{\hbar c}\mathbf{A}_0\right] \tag{8}$$

and

$$\boldsymbol{\Delta}_{nn'}(l-l',t)=\frac{1}{N}\sum_{\mathbf{K}} e^{-i\mathbf{K}\cdot(l-l')}\mathbf{R}_{nn'}\left[\mathbf{K}-\frac{e}{\hbar c}\mathbf{A}_0\right] , \tag{9}$$

where $\mathbf{R}_{nn'}(\mathbf{K})$, the interband coupling parameter, is defined by

$$\mathbf{R}_{nn'}(\mathbf{K})=\frac{i}{\Omega}\int d\mathbf{x}\, U^*_{n\mathbf{K}}\nabla_{\mathbf{K}}U_{n'\mathbf{K}} . \tag{10}$$

Using a simple generalization of the well-known Wannier theorem,[13] Eq. (7) reduces to the differential equation

$$i\hbar\frac{\partial f_n(\mathbf{r},t)}{\partial}=\epsilon_n\left[-i\nabla-\frac{e}{\hbar c}\mathbf{A}_0\right]f_n(\mathbf{r},t) -e\mathbf{E}_0\cdot\sum_{n'}\mathbf{R}_{nn'}\left[-i\nabla-\frac{e}{\hbar c}\mathbf{A}_0\right]f_{n'}(\mathbf{r},t) , \tag{11}$$

where "$\mathbf{r}$" represents an arbitrary lattice position within the crystal. This equation depicts the multiband Wannier envelope function for a Bloch electron in an electric field.

It is clear that the solution to Eq. (11) for $f_n(\mathbf{r},t)$ can be written as

$$f_n(\mathbf{r},t)=\frac{1}{\sqrt{N}}\sum_{\mathbf{K}} e^{-i/\hbar\int_0^t\epsilon_n[\mathbf{K}-(e/\hbar c)\mathbf{A}_0]dt'} \times e^{i\mathbf{K}\cdot\mathbf{r}}A_n(\mathbf{K},t) , \tag{12}$$

where the expansion coefficients, $A_n(\mathbf{K},t)$, satisfy the equations

$$i\hbar\frac{\partial}{\partial t}A_n(t)=-\sum_{n'\neq n}B_{nn'}(t)A_{n'}(t)\ , \tag{13}$$

and where "n" and "n'" index the complete set of energy bands for the crystal. [Note that although A_n and $B_{nn'}$ in Eq. (13) are $\mathbf{K}$ dependent, we use the notation $A_n(t)$ for $A_n(\mathbf{K},t)$, and $B_{nn'}(t)$ for $B_{nn'}(\mathbf{K},t)$ for convenience since Eq. (13) couples A_n and $A_{n'}$ for the same $\mathbf{K}$ value.] In Eq. (13), the time-dependent interband matrix elements $B_{nn'}(t)$ are given by

$$B_{nn'}(t)=e\mathbf{E}_0\cdot\mathbf{R}_{nn'}\left[\mathbf{K}-\frac{e}{\hbar c}A_0\right]e^{-i/\hbar\int_0^t(\epsilon_{n'}-\epsilon_n)dt'}\ , \tag{14}$$

where ϵ_n and $\epsilon_{n'}$ are explicit functions of $\mathbf{K}-(e/\hbar c)\mathbf{A}_0$.

In Sec. III, the properties of $f_n(\mathbf{r},t)$ are discussed within the context of the one-band model, i.e., when $B_{nn'}=0$; in Sec. IV, the envelope functions $f_n(\mathbf{r},t)$ are obtained in a multiband theory through the use of the Wigner-Wiesskopf approximation.

III. ONE-BAND APPROXIMATION

In the one-band approximation, $B_{nn'}=0$ for all "n" and "n'"; it then follows from Eq. (13) that $A_n(t)$ is a constant in time; in this case, A_n is a function of $\mathbf{K}$ alone, established by the initial state of the system, so that the envelope function for a single, uncoupled band (labeled by the superscript "SB") is

$$f_n^{\mathrm{SB}}(l,t)=\frac{1}{\sqrt{N}}\sum_{\mathbf{K}}e^{-i/\hbar\int_0^t\epsilon_n[\mathbf{K}-(e/\hbar c)\mathbf{A}_0]dt'}\times e^{i\mathbf{K}\cdot l}A_n(\mathbf{K},0)\ , \tag{15}$$

where it is noted that all of the time dependence of $f_n^{\mathrm{SB}}(l,t)$ is governed by the $\mathbf{K}$-dependent phase factor. $A_n(\mathbf{K},0)$ can be expressed easily in terms of the initial values of the envelope functions, $f_n(l,0)$, as

$$A_n(\mathbf{K},0)=\frac{1}{\sqrt{N}}\sum_{l'}e^{-i\mathbf{K}\cdot l'}f_n(l',0)\ ; \tag{16}$$

in using $A_n(\mathbf{K},0)$ of Eq. (16) in Eq. (15), it is clear that $f_n^{\mathrm{SB}}(l,t)$ can be written as

$$f_n^{\mathrm{SB}}(l,t)=\sum_{l'}K_n(l-l',t)f_n(l',0)\ , \tag{17}$$

where $K_n(l-l',t)$, the time evolution kernel, is given by

$$K_n(l-l',t)=\frac{1}{N}\sum_{\mathbf{K}'}e^{-i/\hbar\int_0^t\epsilon_n[\mathbf{K}-(e/\hbar c)\mathbf{A}_0]dt'}e^{i\mathbf{K}\cdot(l-l')}\ . \tag{18}$$

The general oscillatory nature of $f_n^{\mathrm{SB}}(l,t)$ in the direction of electric field (x direction) is delineated explicitly by invoking the $\mathbf{K}$-space preiodicity of $\epsilon_n(\mathbf{K})$, namely $\epsilon_n(\mathbf{K})=\epsilon_n(\mathbf{K}+\mathbf{G}_j)$, where the $|\mathbf{G}_j|=j2\pi/a$ are the appropriate reciprocal-lattice vectors. Using this periodicity condition, the time evolution kernel, after an integral number of Bloch periods $s\tau_B$, where τ_B is a Bloch period, have elapsed, becomes

$$\mathbf{K}_n(l-l',s\tau_B)=\delta_{l_x,l_x'}\frac{1}{N_\perp}\sum_{\mathbf{K}_\perp}e^{-(i/\hbar)\bar{\epsilon}_n(\mathbf{K}_\perp)s\tau_B}e^{i\mathbf{K}_\perp\cdot(l-l')_\perp}$$
$$\equiv\delta_{l_x,l_x'}\bar{K}_n(l_\perp-l_\perp',s\tau_B)\ , \tag{19}$$

where

$$\bar{\epsilon}_n(\mathbf{K}_\perp)=\frac{1}{N_x}\sum_{K_x}\epsilon_n(K_x,\mathbf{K}_\perp)\ , \tag{20}$$

the average value of $\epsilon_n(\mathbf{K})$ along the K_x direction in the Brillouin zone, is independent of K_x. Here the subscript "x" indicates the direction of the electric field, and the subscript "$\perp$" indicates the direction perpendicular to the electric field. Therefore, it follows from Eqs. (17) and (19) that

$$f_n^{\mathrm{SB}}(l,s\tau_B)=\sum_{l_\perp'}\bar{K}_n(l_\perp-l_\perp',s\tau_B)f_n(l_x,l_\perp',0)\ , \tag{21}$$

showing that $f_n^{\mathrm{SB}}(l,t)$ oscillates with frequency ω_B, where $\omega_B=eE_0a/\hbar$, in the direction of the electric field, and is diffusive in the direction perpendicular to the electric field, as explicitly shown by the example in Eq. (35).

The oscillatory behavior of $f_n^{\mathrm{SB}}(l,t)$ is clearly seen in the case of one dimension, i.e., $\mathbf{K}_\perp\equiv0$; then

$$K_n(l-l',s\tau_B)=e^{-(i/\hbar)\bar{\epsilon}_n(0)s\tau_B}\delta_{l,l'}\ , \tag{22}$$

where

$$\bar{\epsilon}_n(0)=\frac{1}{N_x}\sum_{\mathbf{K}_x}\epsilon_n(K_x)\ , \tag{23}$$

the average value of $\epsilon_n(K_x)$ over the one-dimensional Brillouin zone, is independent of K_x; in this case, it follows from Eqs. (17) and (22) that

$$f_n^{\mathrm{SB}}(l,s\tau_B)=e^{-(i/\hbar)\bar{\epsilon}_n(0)s\tau_B}f_n(l,0)\ , \tag{24}$$

so that

$$|f_n^{\mathrm{SB}}(l,s\tau_B)|=|f_n(l,0)|\ , \tag{25}$$

where "s" refers to a positive integer. Further, it follows from Eq. (24) that, in the single-band, one-dimensional model, with a given $\epsilon_n(\mathbf{K})$, the total wave function is periodic in time with Bloch frequency up to a constant phase factor in the direction of the field.

The kernel $K_n(l-l',t)$ of Eq. (18) explicitly shows the tendency for localization to set in as the electric field increases. This can be seen by noting, through the use of $\epsilon_n(\mathbf{K})=\sum_l e^{i\mathbf{K}\cdot l}\epsilon_n(l)$, that the integral in the phase factor of the time evolution kernel in Eq. (18) can be further evaluated as

$$-\frac{i}{\hbar}\int_0^t \epsilon_n\left[\mathbf{K}+\frac{e\mathbf{E}_0}{\hbar}t'\right]dt' = -\frac{i}{\hbar}\bar{\epsilon}_n(\mathbf{K}_\perp)t - \sum_{l_x'\neq 0}\frac{(e^{i\omega_B l_x' t}-1)}{\hbar\omega_B l_x'}e^{iK_x a l_x'}\varepsilon_n(l_x',\mathbf{K}_\perp)\ , \tag{26}$$

where

$$\varepsilon_n(l_x,\mathbf{K}_\perp)\equiv\sum_{l_\perp'}\varepsilon_n(l_x',l_\perp')e^{i\mathbf{K}_\perp\cdot l_\perp'}\ , \tag{27}$$

so that, in the high-field limit, as $\hbar\omega_B \gg \varepsilon_n(\mathbf{a})$,

$$e^{-i/\hbar\int_0^t\epsilon_n[\mathbf{K}+(eE_0/\hbar)t']dt'}\approx e^{-(i/\hbar)\bar{\epsilon}_n(\mathbf{K}_\perp)t}\left\{1-\sum_{l_x'}\frac{\varepsilon_n(l_x',\mathbf{K}_\perp)}{\hbar\omega_B l_x'}e^{iK_x a l_x'}[e^{i\omega_B l_x' t}-1]+O(\omega_B^{-2})\right\}. \tag{28}$$

Putting Eq. (28) into Eq. (18), and using the completeness relation, we obtain the three-dimensional time evolution kernel for general band $\epsilon_n(\mathbf{K})$ in the high-field limit as

$$K_n(\boldsymbol{l}-\boldsymbol{l}',t)=\frac{1}{N_\perp}\sum_{\mathbf{K}_\perp}e^{-(i/\hbar)\bar{\epsilon}_n(\mathbf{K}_\perp)t}e^{i\mathbf{K}_\perp\cdot(\boldsymbol{l}-\boldsymbol{l}')_\perp}\left\{\delta_{l_x,l_x'}+\frac{2\varepsilon_n(l_x-l_x',\mathbf{K}_\perp)}{\hbar\omega_B(l_x-l_x')}\sin\left[\frac{l_x-l_x'}{2}\omega_B t\right]e^{i[(\pi/2)(l_x-l_x')/(2)\omega_B t)]}(1-\delta_{l_x l_x'})\right\}. \tag{29}$$

In the one-dimensional case, Eq. (29) is simplified as

$$K_n(l-l',t)=e^{-(i/\hbar)\bar{\epsilon}_n(0)t}\left[\delta_{l,l'}+\frac{2\varepsilon_n(l-l')}{\hbar\omega_B(l-l')}\sin\left[\frac{l-l'}{2}\omega_B t\right]e^{i[(\pi/2)-(l-l')/(2)\omega_B t]}(1-\delta_{l,l'})\right]. \tag{30}$$

For the familiar nearest-neighbor tight-binding approximation of a linear-chain model,

$$\epsilon_n(\mathbf{K})=\epsilon_n(0)+W\sin^2\frac{\mathbf{K}\cdot\mathbf{a}}{2}\ , \tag{31}$$

with "**a**" denoted as the basic lattice vector in a specific crystallographic direction, and with $\epsilon_n(0)$ and "W" denoted as the energy-band minimum and width, respectively. For this model, the time evolution kernel of Eq. (18) can be evaluated with no approximations to give

$$K_n(l-l',t)=e^{-i[\varepsilon_n(0)/\hbar]t-i(l-l')[(\pi/2)+(1/2)\omega_B t]}\times J_{l-l'}\left[\frac{W}{\hbar\omega_B}\sin(\tfrac{1}{2}\omega_B t)\right], \tag{32}$$

where $J_{l-l'}$ is a Bessel function of the first kind.[14] $k_n(l-l',t)$ of Eq. (32) reduces to Eq. (30) in the limit of high electric field. Thus for the one-dimensional, nearest-neighbor, tight-binding approximation,

$$f_n^{\mathrm{SB}}(l,t)=\sum_{l'}e^{-i[\varepsilon_n(0)/\hbar]t-i(l-l')[(\pi/2)+(1/2)\omega_B t]}\times J_{l-l'}\left[\frac{W}{\hbar\omega_B}\sin(\tfrac{1}{2}\omega_B t)\right]f_n(l',0)\ . \tag{33}$$

In the limit of high electric field, that is, for the $|W/\hbar\omega_B|\ll 1$, the absolute value of argument of the Bessel function in Eq. (33) is much less than 1, and the Bessel function $J_{l-l'}$ tends to be localized about $l\approx l'$ since $J_{l-l'}(\xi)$ tends to $\delta_{l,l'}$ as ξ tends to zero. It is clear that the single-band model leads to localization of the electron in high fields, that is fields such that $(l-l')\hbar\omega_B \gg \varepsilon_n(l-l')$; it is also clear that conduction occurs through hopping from site to site as evidenced in Eq. (30).

The time evolution kernel can also be derived exactly for the three-dimensional (3D) simple cubic lattice in the nearest-neighbor tight-binding approximation. The energy-band function for the 3D simple cubic lattice is given by

$$\epsilon_n(\mathbf{K})=\varepsilon_n(0)+2\varepsilon_n(a)[\cos(K_x a)+\cos(K_y a)+\cos(K_z a)]\ , \tag{34}$$

where $\varepsilon_n(a)$ is the nearest-neighbor interaction energy. The time evolution kernel of Eq. (18) is

$$K_n(l-l',t)=e^{-i[\varepsilon_n(0)+(\omega_B/2)(l_x-l_x')]t}J_{l_x-l_x'}\left[\frac{4\varepsilon_n(a)}{\hbar\omega_B}\sin\tfrac{1}{2}\omega_B t\right]\times J_{l_y-l_y'}\left[\frac{2\varepsilon_n(a)}{\hbar}t\right]J_{l_z-l_z'}\left[\frac{2\varepsilon_n(a)}{\hbar}t\right]e^{-i(\pi/2)(l_x+l_y+l_z-l_x'-l_y'-l_z')}\ ; \tag{35}$$

$J_{l_x-l_x'}$ in Eq. (35) shows clearly the tendency for electron to localize in the direction of electric field (x direction) in the high-electric-field limit, since $J_{l_x-l_x'}$ tends to $\delta_{l_x l_x'}$ as the argument of the Bessel function tends to zero. Further, the Bessel functions in the "y" and the "z" directions introduce diffusion in the direction perpendicular to the electric field, since the arguments of the Bessel functions are proportional to the time "t."

IV. MULTIBAND ANALYSIS USING WIGNER-WEISSKOPF APPROXIMATION

In the multiband analysis, the envelope function is given by Eq. (12), with band-coupling dependence reflected in the coefficients, $A_n(\mathbf{K},t)$, given by Eq. (13). Since the set of equations given in Eq. (13) is not solvable exactly with most approximate analytical methods addressing the short-time behavior, we use the Wigner-Weisskopf approximation to establish the long-time behavior of $A_n(\mathbf{K},t)$ in Eq. (13). In the Wigner-Weisskopf approximation,[11] the equation for the A_n is written as

$$i\hbar\frac{\partial}{\partial t}A_n(t)=-\sum_{n'\neq n}B_{nn'}(t)A_{n'}(t)\ , \tag{36}$$

with all other $A_{n'}$ satisfying the approximate equation

$$i\hbar\frac{\partial}{\partial t}A_{n'}(t)=-B_{n'n}(t)A_n(t)=-B^*_{nn'}(t)A_n(t)\ ; \tag{37}$$

both $A_n(\mathbf{K},t)$ and $B_{nn'}(\mathbf{K},t)$ are implicit functions of the same $\mathbf{K}$ value, therefore the $\mathbf{K}$ dependence in A_n and $B_{nn'}$ is suppressed unless specially needed. In essence, the approximation couples the state of interest "n" to all other states of the system "n'" while including only direct reflective feedback from the states "n'" to the state of interest, thereby ignoring multiple probability reflections. In addition, the above approximation guarantees conservation of probability, since it can easily be shown that[15]

$$|A_n|^2+\sum_{n'\neq n}|A_{n'}|^2=1 \tag{38}$$

for A_n and $A_{n'}$.

We solve for the A_n and $A_{n'}$ of Eqs. (36) and (37) subject to the initial band occupation conditions

$$A_n(0)=1\ ,\quad A_{n'}(0)=0\ ,\quad n'\neq n\ . \tag{39}$$

In Bloch dynamics, several Bloch periods is the time scale for very early time development, while Zener tunneling times set the scale for the long-time development.[2] In this analysis, we focus on the long-time temporal behavior, so that initial transient effects will be ignored throughout the analysis.

In solving for A_n and $A_{n'}$ in Eqs. (36) and (37), subject to (39), we integrate Eq. (37) and substitute $A_{n'}$ into Eq. (36) to obtain

$$\frac{\partial}{\partial t}A_n(t)=-\frac{1}{\hbar^2}\sum_{n'\neq n}B_{nn'}(t)\int_0^t B^*_{nn'}(t')A_n(t')dt'\ . \tag{40}$$

In essence, the Wigner-Weisskopf approximation uncouples the system of equations for the amplitudes $\{A_n\}$, resulting in an integrodifferential equation for $A_n(t)$ alone.

Substituting $B_{nn'}$ given by Eq. (14) into Eq. (40), we obtain

$$\frac{\partial}{\partial t}\mathbf{A}_n(t)=-\sum_{n'\neq n}\left[\frac{eE_0}{\hbar}\right]^2 X_{nn'}(t)e^{-i/\hbar\int_0^t(\epsilon_{n'}-\epsilon_n)dt'}\int_0^t X^*_{nn'}(t')e^{i/\hbar\int_0^{t'}(\epsilon_{n'}-\epsilon_n)dt''}A_n(t')dt'\ , \tag{41}$$

where $X_{nn'}$ is the component of $\mathbf{R}_{nn'}$ in the direction of the electric field.

In Appendix A of this paper, we show that, for $t\geq 10\tau_B$, the integral phase factor in Eq. (41) can be expressed in terms of time-dependent and time-independent components as

$$-\frac{i}{\hbar}\int_0^t\epsilon_n dt'\approx-\frac{i}{\hbar}\bar{\epsilon}_n(\mathbf{K}_\perp)t+\eta_n(\mathbf{K})\ , \tag{42}$$

where $\bar{\epsilon}_n(\mathbf{K}_\perp)$, the average value of the energy-band function $\epsilon_n(\mathbf{K})$ in the direction of the electric field, is given by Eq. (20), and $\eta_n(\mathbf{K})$ is given by

$$\eta_n(\mathbf{K})=\sum_{l_x\neq 0}\frac{\epsilon_n(l_x,\mathbf{K}_\perp)}{\hbar\omega_B l_x}e^{iK_x a l_x}\ , \tag{43}$$

and is independent of time.

Using

$$X_{nn'}(t)=\sum_l\Delta_{nn'}(l)e^{i\mathbf{K}\cdot l+i(e\mathbf{E}_0\cdot l)t}=\sum_l\Delta_{nn'}(l)e^{i\mathbf{K}\cdot l+i\omega_B l_x t}\ ,$$

where $\omega_B=eE_0a/\hbar$ (angular frequency of Bloch oscillation, where "a" is the lattice spacing), and using Eq. (42) in Eq. (41) while letting $\omega_{nn'}(\mathbf{K}_\perp)=\epsilon_{nn'}(\mathbf{K}_\perp)/\hbar$, with $\epsilon_{nn'}(\mathbf{K}_\perp)=\bar{\epsilon}_{n'}(\mathbf{K}_\perp)-\bar{\epsilon}_n(\mathbf{K}_\perp)$, we express Eq. (41) in terms of $\Delta_{nn'}(l)$ as

$$\frac{\partial}{\partial t}A_n(t)=-\sum_{n'\neq n}\left[\frac{eE_0}{\hbar}\right]^2\sum_{l,l'}\Delta_{nn'}(l)\Delta^*_{nn'}(l')e^{i\mathbf{K}\cdot(l-l')+i\omega_B(l_x-l_x')t}\int_0^t e^{i[\omega_B l_x'-\omega_{nn'}(\mathbf{K}_\perp)](t-t')}A_n(t')dt'\ . \tag{44}$$

Equation (44) may be solved through the use of Laplace transforms. In noting that

$$a_n(s)=\int_0^\infty e^{-st}A_n(t)dt\equiv L\{A_n(t)\}\ , \tag{45}$$

the Laplace transform of (44) is

$$sa_n(s)-A_n(0)=-\sum_{n'\neq n}\left[\frac{eE_0}{\hbar}\right]^2\sum_{l,l'}\Delta_{nn'}(l)\Delta^*_{nn'}(l')e^{i\mathbf{K}\cdot(l-l')}\frac{a_n[s-i\omega_B(l_x-l'_x)]}{[s-i\omega_B l_x+i\omega_{nn'}(\mathbf{K}_\perp)]}\ . \tag{46}$$

The sum on the right-hand side of the equation shows the explicit time dependence on the Stark-ladder spectrum as indicated in the terms $a_n[s-i\omega_B(l_x-l'_x)]$. Separating the summation on the right-hand side of the equation into two parts, one with $l_x=l'_x$ terms, and the other with $l_x\neq l'_x$ terms, we obtain

$$\begin{aligned}sa_n(s)-A_n(0)=-\left[\frac{eE_0}{\hbar}\right]^2\sum_{n'\neq n}\Bigg\{&\sum_{l_x}\sum_{l_\perp}\sum_{l'_\perp}\Delta_{nn'}(l_x,l_\perp)\Delta_{nn'}(l_x,l'_\perp)e^{i\mathbf{K}_\perp\cdot(l_\perp-l'_\perp)}\frac{a_n(s)}{[s-i\omega_B l_x+i\omega_{nn'}(\mathbf{K}_\perp)]}\\&+\sum_{\substack{l\\ l_x\neq l'_x}}\sum_{l'}\Delta_{nn'}(l)\Delta^*_{nn'}(l')e^{i\mathbf{K}\cdot(l-l')}\frac{a_n[s-i\omega_B(l_x-l'_x)]}{[s-i\omega_B l_x+i\omega_{nn'}(\mathbf{K}_\perp)]}\Bigg\}\ .\end{aligned} \tag{47}$$

Noting that the inverse Laplace transform of $a_n[s-i\omega_B(l_x-l'_x)]$ is $\exp[i\omega_B(l_x-l'_x)t]A_n(t)$, corresponding to rapidly oscillatory terms for $l_x\neq l'_x$ and as $\omega_B t\gg 1$, the first summation, containing $l_x=l'_x$ terms only, dominates in the long-time limit. Therefore, as an approximation, we suppress the $l_x\neq l'_x$ terms; then the Laplace transform of $A_n(t)$, $a_n(s)$, can be expressed explicitly as a function of "s" as

$$a_n(s)=A_n(0)\left[s+\sum_{n\neq n}\left[\frac{eE_0}{\hbar}\right]^2\sum_{l_x}|D_{nn'}(l_x,\mathbf{K}_\perp)|^2\frac{1}{s-i\omega_B l_x+i\omega_{nn'}(\mathbf{K}_\perp)}\right]^{-1}\ , \tag{48}$$

where

$$D_{nn'}(l_{x'},\mathbf{K}_\perp)=\sum_{l_\perp}\Delta_{nn'}(l_x,l_\perp)e^{i\mathbf{K}_\perp\cdot l_\perp}\ . \tag{49}$$

$A_n(t)$ is then obtained by the inverse Laplace transform

$$\begin{aligned}A_n(t)&=\frac{1}{2\pi i}\int_{\epsilon-i\infty}^{\epsilon+i\infty}a_n(s)e^{st}ds\\&=\frac{A_n(0)}{2\pi i}\int_{\epsilon-i\infty}^{\epsilon+i\infty}\left[s+\sum_{n'\neq n}\left[\frac{eE_0}{\hbar}\right]^2\sum_{l_x}|D_{nn'}(l_x,\mathbf{K}_\perp)|^2\frac{1}{s+i[-\omega_B l_x+\omega_{nn'}(\mathbf{K}_\perp)]}\right]^{-1}e^{st}ds\ ,\end{aligned} \tag{50}$$

where "s" is a complex variable in the integrand, ϵ is a small positive number, and the path of integration is parallel to the imaginary axis. Setting $s=\epsilon+iy$, the integral is reduced to an integral over the real axis, and $A_n(t)$ can be written as

$$A_n(t)=\frac{A_n(0)}{2\pi i}\lim_{\epsilon\to 0}\int_{-\infty}^{\infty}\frac{e^{\epsilon t}e^{iyt}dy}{y-i\epsilon-\sum_{n'\neq n}\left[\frac{eE_0}{\hbar}\right]^2\sum_{l_x}|D_{nn'}(l_x,\mathbf{K}_\perp)|^2\frac{1}{y-\omega_B l_x+\omega_{nn'}(\mathbf{K}_\perp)-i\epsilon}}\ . \tag{51}$$

In ignoring "y" in the sum of the denominator of the integrand, which effectively suppresses the time development of $A_n(t)$ in the first several Bloch periods,[11,15] and using the Poisson sum formula[16] for the sum while using $\lim_{\epsilon\to 0}(1)/(x-i\epsilon)=P(1/x)+i\pi\delta(x)$ for the residual portion, the summation in the denominator of the integrand can be expressed in terms of a real part with the principal value, and an imaginary part with a δ function (see Appendix B), as

$$\lim_{\epsilon\to 0}\sum_{n'\neq n}\left[\frac{eE_0}{\hbar}\right]^2\sum_{l_x}|D_{nn'}(l_x,\mathbf{K}_\perp)|^2\frac{1}{-\omega_B l_x+\omega_{nn'}(\mathbf{K}_\perp)-i\epsilon}=\Delta\omega_n(\mathbf{K}_\perp)+i\frac{\gamma_n(\mathbf{K}_\perp)}{2}\ , \tag{52}$$

where

$$\Delta\omega_n(\mathbf{K}_\perp)=\left[\frac{eE_0}{\hbar}\right]^2\sum_{n'\neq n}\sum_{l_x}|D_{nn'}(l_x,\mathbf{K}_\perp)|^2P\frac{1}{-\omega_B l_x+\omega_{nn'}(\mathbf{K}_\perp)} \tag{53}$$

and

$$\frac{\gamma_n(\mathbf{K}_\perp)}{2}=\pi\frac{1}{\omega_B}\left[\frac{eE_0}{\hbar}\right]^2\sum_{n'\neq n}|D_{nn'}(l_{nn'}(\mathbf{K}_\perp),\mathbf{K}_\perp)|^2 . \tag{54}$$

It is noted in Eq. (54) that $l_{nn'}(\mathbf{K}_\perp)=\omega_{nn'}(\mathbf{K}_\perp)/\omega_B=\epsilon_{nn'}(\mathbf{K}_\perp)/eE_0a$. Thus it follows from Eqs. (51) and (52) that

$$A_n(\mathbf{K},t)\approx A_n(\mathbf{K},0)\int_{-\infty}^{\infty}\frac{e^{iyt}dy}{y-\Delta\omega_n(\mathbf{K}_\perp)-i(\gamma_n(\mathbf{K}_\perp)/2)}=A_n(\mathbf{K},0)e^{\{i\Delta\omega_n(\mathbf{K}_\perp)-[\gamma_n(\mathbf{K}_\perp)/2]\}t} . \tag{55}$$

Note that $\Delta\omega_n$ and γ_n are $\mathbf{K}_\perp$ dependent, so that $|A_n(\mathbf{K},t)|^2=|A_n(\mathbf{K},0)|^2\exp[-\gamma_n(\mathbf{K}_\perp)t]$, $|A_n(\mathbf{K},t)|^2$ decays exponentially with a decay rate of $\gamma_n(\mathbf{K}_\perp)$. Using the result of Eq. (55) in Eq. (12), the envelope function for the initial band "n" is

$$\begin{aligned}f_n(\boldsymbol{l},t)&=\frac{1}{\sqrt{N}}\sum_{\mathbf{K}}e^{-i/\hbar\int_0^t\epsilon_n[\mathbf{K}-(e/\hbar c)\mathbf{A}_0]dt'}e^{i\mathbf{K}\cdot\boldsymbol{l}}e^{\{i\Delta\omega_n(\mathbf{K}_\perp)-[\gamma_n(\mathbf{K}_\perp)/2]\}t}A_n(\mathbf{K},0)\\&=\sum_{l'}\left\{\frac{1}{N_\perp}\sum_{\mathbf{K}}e^{-i/\hbar\int_0^t\epsilon_n[\mathbf{K}-(e/\hbar c)\mathbf{A}_0]dt'}e^{i\mathbf{K}\cdot(\boldsymbol{l}-\boldsymbol{l}')}e^{\{i\Delta\omega_n(\mathbf{K}_\perp)-[\gamma_n(\mathbf{K}_\perp)/2]\}t}\right\}f_n(\boldsymbol{l}',0) ,\end{aligned} \tag{56}$$

where the term inside the parentheses of Eq. (56) is the time evolution kernel for the initial band; this kernel differs from the single-band kernel of Eq. (18) due to the presence of the $\mathbf{K}_\perp$-dependent attenuation factor involving $\Delta\omega_n(\mathbf{K}_\perp)$ and $\gamma_n(\mathbf{K}_\perp)$. It then follows that for an electron initially placed in a localized Wannier state, i.e., $f_n(\boldsymbol{l}',0)=\delta_{\boldsymbol{l}',\boldsymbol{l}_0}$, the envelope function becomes, after "s" Bloch periods,

$$f_n(\boldsymbol{l},s\tau_B)=\delta_{l_x,l_{0x}}\frac{1}{N_\perp}\sum_{\mathbf{K}_\perp}e^{[-(i/\hbar)\bar{\epsilon}_n(\mathbf{K}_\perp)+i\Delta\omega_n(\mathbf{K}_\perp)-\gamma_n(\mathbf{K}_\perp)/2]s\tau_B}e^{i\mathbf{K}_\perp\cdot(\boldsymbol{l}_\perp-\boldsymbol{l}'_\perp)} . \tag{57}$$

Further, when the electron is subjected to mixed initial conditions, i.e., a Wannier-like state in the x direction, and Bloch states in the $\perp$ direction, then

$$A_n(\mathbf{K},0)=\frac{1}{\sqrt{N_x}}e^{-iK_xl_{0x}}\delta_{\mathbf{K}_\perp,\mathbf{K}_{0\perp}} , \quad f_n(\boldsymbol{l},0)=\delta_{l_x,l_{0x}}\frac{1}{\sqrt{N_\perp}}e^{i\mathbf{K}_{0\perp}\cdot\boldsymbol{l}_\perp} . \tag{58}$$

In this case, after "s" Bloch periods, the envelope function of initial state (58) evolves to

$$f_n(\boldsymbol{l},s\tau_B)=\delta_{l_x,l_{0x}}\frac{1}{\sqrt{N_\perp}}e^{\{-(i/\hbar)\bar{\epsilon}_n(\mathbf{K}_{0\perp})+i\Delta\omega_n(\mathbf{K}_{0\perp})-[\gamma_n(\mathbf{K}_{0\perp})/2]\}s\tau_B}e^{i\mathbf{K}_{0\perp}\cdot\boldsymbol{l}_\perp} , \tag{59}$$

which exhibits the periodicity in the x direction, and exponential decay out of the initial band at time $s\tau_B$.

The probability for an electron to be in its initial band "n" after time "t" is

$$\begin{aligned}\rho_n(t)&=\sum_{\boldsymbol{l}}|f_n(\boldsymbol{l},t)|^2\\&=\sum_{\mathbf{K}}|A_n(\mathbf{K},t)|^2=\sum_{\mathbf{K}}|A_n(\mathbf{K},0)|^2e^{-\gamma_n(\mathbf{K}_\perp)t} ,\end{aligned} \tag{60}$$

where the exponential terms indicate the irreversible decay out of nth band into the upper bands of the crystal due to the power absorbed by the electric field. Thus the total transition rate for an electron in initial band "n" is

$$\begin{aligned}\Gamma_n(t)\equiv-\frac{\partial\rho_n(t)}{\partial t}&=-\frac{\partial}{\partial t}\sum_{\mathbf{K}}|A_n(\mathbf{K},0)|^2e^{-\gamma_n(\mathbf{K}_\perp)t}\\&=\sum_{\mathbf{K}}\gamma_n(\mathbf{K}_\perp)|A_n(\mathbf{K},0)|^2e^{-\gamma_n(\mathbf{K}_\perp)t} .\end{aligned} \tag{61}$$

For $\gamma_n(\mathbf{K}_\perp)t\leq 1$, the transition rate is approximated by

$$\Gamma_n(t)\approx\Gamma_n(0)=\sum_{\mathbf{K}}|A_n(\mathbf{K},0)|^2\gamma_n(\mathbf{K}_\perp) . \tag{62}$$

This transition rate is the total transition probability per unit time for an electron to tunnel out of state "n" while coupled to all other bands. Thus the time of Zener tunneling, τ_z, is determined by

$$\tau_z \equiv \frac{1}{\Gamma_n(0)} = \frac{1}{\sum_{\mathbf{K}} |A_n(\mathbf{K},0)|^2 \gamma_n(\mathbf{K}_\perp)} = \frac{a^2}{(2\pi)^2} \frac{\tau_B}{\sum_{\mathbf{K}} |A_n(\mathbf{K},0)|^2 \sum_{n' \neq n} |D_{nn'}(l'_{nn'}(\mathbf{K}_\perp),\mathbf{K}_\perp)|^2} . \tag{63}$$

It is interesting to note that the total transition rate (or the Zener tunneling time) depends not only on $\gamma_n(\mathbf{K}_\perp)$, but also on the initial conditions $A_n(\mathbf{K},0)$. In the following, we examine the dependence of $\Gamma_n(0)$ on the initial conditions. First, for initial conditions based on localized states, i.e., Wannier states,

$$f_n(l,0)=\delta_{l,l_0}, \quad A_n(\mathbf{K},0)=\frac{1}{\sqrt{N}} e^{-i\mathbf{K}\cdot l_0} , \tag{64}$$

so that the total transition rate from Eq. (62) is

$$\Gamma_n(0)=\frac{1}{N}\sum_{\mathbf{K}} \gamma_n(\mathbf{K}_\perp) \equiv \frac{1}{N_\perp}\sum_{\mathbf{K}_\perp} \gamma_n(\mathbf{K}_\perp) , \tag{65}$$

the average value of $\gamma_n(\mathbf{K}_\perp)$ over the entire $\mathbf{K}$ space of the Brillouin zone. However, for initial conditions based on Bloch states, i.e.,

$$f_n(l,0)=\frac{1}{\sqrt{N}} e^{i\mathbf{K}_0\cdot l}, \quad A_n(\mathbf{K},0)=\delta_{\mathbf{K},\mathbf{K}_0} , \tag{66}$$

the total transition rate from Eq. (62) is

$$\Gamma_n(0)=\sum_{\mathbf{K}} \gamma_n(\mathbf{K}_\perp)\delta_{\mathbf{K},\mathbf{K}_0} \equiv \gamma_n(\mathbf{K}_{0\perp}) . \tag{67}$$

Finally, for initially mixed states of Eq. (58), the total transition rate is simply

$$\Gamma_n(0)=\gamma_n(\mathbf{K}_{0\perp}) , \tag{68}$$

the decay rate for $\mathbf{K}_\perp=\mathbf{K}_{0\perp}$. In comparing $\Gamma_n(0)$ from Eqs. (67) and (68), it is clear that when the initial state in the direction of the field is a Bloch state, the associated tunneling times are identical.

Note that $D_{nn'}(l_x,\mathbf{K}_\perp)$ defined in Eq. (49) can also be expressed as

$$D_{nn'}(l_x,\mathbf{K}_\perp)=\frac{1}{N_x}\sum_{K_x} X_{nn'}(\mathbf{K}) e^{-iK_x a l_x} ; \tag{69}$$

we show in Appendix C, by utilizing the analytic properties of $X_{nn'}(\mathbf{K})$, $\epsilon_n(\mathbf{K})$, and $\epsilon_{n'}(\mathbf{K})$ based on the analytic continuation of energy bands belonging to "n" and "n'" in the complex K_x plane, that

$$D_{n,n'}(l_x,\mathbf{K}_\perp)=\frac{i}{4} a e^{-q_{nn'}a|l_x|} , \tag{70}$$

where $q_{nn'}=|q|$, with "q" determined by $\epsilon_n(q,\mathbf{K}_\perp)=\epsilon_{n'}(q,\mathbf{K}_\perp)$. Therefore, the field dependence of $\gamma_n(K_\perp)$ of Eq. (54) is

$$\gamma_n(\mathbf{K}_\perp)=\frac{\pi}{8}\omega_B \sum_{n' \neq n} e^{-2q_{nn'}(\mathbf{K}_\perp)a[\epsilon_{nn'}(\mathbf{K}_\perp)/|eE_0 a|]} , \tag{71}$$

so that it follows from Eq. (63) that τ_z is generally given by

$$\tau_z = \left[\frac{2}{\pi}\right]^2 \tau_B \left[\sum_{\mathbf{K}} |A_n(\mathbf{K},0)|^2 \sum_{n' \neq n} e^{-2q_{nn'}(\mathbf{K}_\perp)a[\epsilon_{nn'}(\mathbf{K}_\perp)/|eE_0 a|]}\right]^{-1} . \tag{72}$$

It is also noted that $\epsilon_{nn'}(\mathbf{K}_\perp)$ is the average value of the energy-band difference between states "n" and "n'" taken over the direction K_x [the direction of the electric field, as defined above Eq. (44)] in the Brillouin zone. Since the electric-field dependence in Eq. (72) appears in the exponent as well as in the prefactor, τ_z is very sensitive to the field.

For purposes of illustrating how one proceeds from Eq. (72) for a specific band structure, we consider the familiar nearest-neighbor tight-binding model for a simple cubic lattice with band dispersion

$$\epsilon_n(\mathbf{K})=\varepsilon_n(0) \mp 2|\varepsilon_n(a)|[\cos(K_x a)+\cos(K_y a)+\cos(K_z a)] , \tag{73}$$

where "$\mp$" signs corresponds to conduction- or valence-band alternatives. For the bands of Eq. (73), we find that

$$q_{nn'}a=\cosh^{-1}\left\{1+\frac{E_g+4\varepsilon_{nn'}(a)\left[\sin^2\frac{K_y a}{2}+\sin^2\frac{K_z a}{2}\right]}{2\varepsilon_{nn'}(a)}\right\} , \tag{74}$$

where E_g is the energy gap between two bands at $\mathbf{K}=0$, $\varepsilon_{nn'}(a)=\varepsilon_{n'}(a)-\varepsilon_n(a)$, and $q_{nn'}$ is $\mathbf{K}_\perp$ dependent.

The formalism is much more simplified for the one-dimensional model. Since $\Delta\omega_n$ and γ_n are $\mathbf{K}$ independent for the one-dimensional case, the envelope function for the initial band "n" is related to the single-band result as

$$f_n(l,t)=e^{[i\Delta\omega_n-(\gamma_n/2)]t} f_n^{\mathrm{SB}}(l,t) . \tag{75}$$

Therefore, the probability of the electron at initial band "n" and site "l" is

$$|f_n(l,t)|^2=|f_n^{\mathrm{SB}}(l,t)|^2e^{-\gamma_n t}\ . \tag{76}$$

The probability of the electron remaining in its initial band after time "t" is then given by $\rho_n(t)=\sum_{\mathbf{K}}|A_n(\mathbf{K},t)|^2=\sum_{\mathbf{K}}|A_n(\mathbf{K},0)|^2e^{-\gamma_n t}=e^{-\gamma_n t}$, which irreversibly decays into the upper bands of the crystal with a decay rate of γ_n, and the Zener tunneling time is $\tau_z\equiv 1/\gamma_n$.

For a general band structure in a one-dimensional model, the total transition rate for an electron transmitted from initial band "n" of Eq. (71) reduces to

$$\gamma_n=\frac{\pi eE_0a}{8\hbar}\sum_{n'\neq n}\exp\left[-2q_{nn'}a\frac{\epsilon_{nn'}}{eE_0a}\right]\ . \tag{77}$$

Since the average band gap $\epsilon_{nn'}$ increases as the band "n'" increases from initial band "n," the maximum contribution arises from the nearest band "$n'=n+1$"; if the other bands are far away from the initial band, then the decay rate can be approximated by a two-band model, which is

$$\gamma_n=\frac{\pi eE_0a}{8\hbar}\exp\left[-2q_{nn'}a\frac{\epsilon_{nn'}}{eE_0a}\right]\ . \tag{78}$$

For the nearest-neighbor tight-binding approximation, $q_{nn'}a=\cosh^{-1}[1+2E_g^{nn'}/(W_n+W_{n'})]$, where $E_g^{nn'}$ is the gap at $K=0$, and W_n and $W_{n'}$ are respective bandwidths. It is noted that $q_{nn'}a$ and $\epsilon_{nn'}$ can be expressed in terms of the central and zone boundary band gaps. In general, the zone boundary band gap $\varepsilon_g^{nn'}$ can be expressed as $\varepsilon_g^{nn'}=E_g^{nn'}+(W_n+W_{n'})$; for the specific one-dimensional, nearest-neighbor tight-binding model, $\epsilon_{nn'}=(E_g^{nn'}+\varepsilon_g^{nn'})/2$. Thus γ_n of Eq. (78) can be written in the form

$$\gamma_n=\frac{\pi}{8}\omega_Be^{-2C(E_g/\hbar\omega_B)}\ , \tag{79}$$

where $C\equiv C_{\mathrm{ENNTB}}$ is expressed as

$$C_{\mathrm{ENNTB}}=\frac{1}{2}\left[\frac{1+E_g/\varepsilon_g}{E_g/\varepsilon_g}\right]\cosh^{-1}\left[\frac{1+E_g/\varepsilon_g}{1-E_g/\varepsilon_g}\right]\ . \tag{80}$$

In Eq. (80), C_{ENNTB} refers to the coefficient "C" for the exact nearest-neighbor tight-binding (ENNTB) model.

In order to compare the nearest-neighbor tight-binding results to those of other well-known models, we calculate the Zener tunneling transition rate γ_n of Eq. (78) for the effective-mass limit of nearest-neighbor tight-binding theory; γ_n for Kane's two-band model[12] is also presented for comparison purposes. In effective-mass theory, the dispersion curves for ϵ_n and $\epsilon_{n'}$ are given by

$$\begin{aligned}\epsilon_n(\mathbf{K})&=\epsilon_n(0)-\frac{\hbar^2}{2m_n}K^2\\ \epsilon_{n'}(\mathbf{K})&=\epsilon_{n'}(0)+\frac{\hbar^2}{2m_{n'}}K^2\ ,\end{aligned} \tag{81}$$

so that from $\epsilon_n(q)=\epsilon_{n'}(q)$, we see that $q=i(\sqrt{2E_gm_r}/\hbar)$, then γ_n in Eq. (78) becomes

$$\gamma_n=\frac{\pi}{8}\omega_B\exp\left[-2\frac{\frac{a}{\hbar}\sqrt{2m_rE_g}\epsilon_{nn'}}{\hbar\omega_B}\right]\ , \tag{82}$$

where m_r is the reduced mass defined by $(1/m_r)=(1/m_n)+(1/m_{n'})$ and, E_g is the band gap at $K=0$.

In the effective-mass limit of nearest-neighbor tight binding, it is observed that $(\hbar^2/2m_n)=(a^2/4)W_n$, where "$a$" is the one-dimensional lattice constant, and W_n is the bandwidth for band "n". Thus $(1/m_r)=\frac{1}{2}(a/\hbar)^2(W_n+W_{n'})\equiv\frac{1}{2}(a/\hbar)^2(\varepsilon_g^{nn'}-E_g^{nn'})$, so that

$$C_{\mathrm{EMNNTB}}=\left[\frac{1+E_g/\varepsilon_g}{E_g/\varepsilon_g}\right]\left[\frac{E_g/\varepsilon_g}{1-E_g/\varepsilon_g}\right]^{1/2}\ , \tag{83}$$

where C_{EMNNTB} refers to the coefficient "C" for the effecitve-mass limit of the nearest-neighbor tight-binding (EMNNTB) model.

In applying the $\mathbf{k}\cdot\mathbf{P}$ method in the two-band model, Kane obtains[12]

$$\begin{aligned}\epsilon_n(\mathbf{K})&=\frac{E_g}{2}+\frac{\eta}{2}+\frac{\hbar^2K^2}{2m}\\ \epsilon_n(\mathbf{K})&=\frac{E_g}{2}-\frac{\eta}{2}+\frac{\hbar^2\mathbf{K}^2}{2m}\ ,\end{aligned} \tag{84}$$

where $\eta=\sqrt{E_g^2+(E_g/m_r)\hbar^2K^2}$. Solving $\epsilon_n(q)=\epsilon_{n'}(q)$ for q results in $q=i(\sqrt{E_gm_r}/\hbar)$; using an analysis based on the Golden rule, Kane obtains

$$\gamma_n=\frac{\pi}{18}\omega_B\exp\left[-2\frac{\frac{\pi}{4}\frac{a}{\hbar}\sqrt{m_rE_g}E_g}{\hbar\omega_B}\right]\ , \tag{85a}$$

which is significantly different in both exponential and preexponential factors from the results obtained for the exact nearest-neighbor tight-binding model and the effective-mass limit of the nearest-neighbor tight-binding model as indicated in Eqs. (79), (80), and (83). Aside from the differing prefactor of $\frac{4}{9}$ in Eq. (85a), the results for Kane's two-band model also fit into the form of Eq. (79), where C is given by

$$C_{\mathrm{Kane}}=\frac{\pi}{4}\left[\frac{a}{\hbar}\right]\sqrt{m_rE_g}\ . \tag{85b}$$

If m_r is chosen to be identical to that of the EMNNTB reduced mass value, i.e., $\sqrt{m_r}=\sqrt{2}(\hbar/a)(1/\sqrt{\varepsilon_g-E_g})$, then C_{Kane} in Eq. (85b) becomes

$$C_{\mathrm{Kane}}=\frac{\pi}{\sqrt{8}}\left[\frac{E_g/\varepsilon_g}{1-E_g/\varepsilon_g}\right]^{1/2}\ . \tag{85c}$$

A comparison of γ_n for the ENNTB, EMNNTB, and Kane models is instructive in showing the significant variation in the exponential dependence of E_g/ε_g for the three cases, and how the variation in band-structure parameters markedly effects the magnitude of the transition rate γ_n for each case. As observed in Fig. 1, in general,

$\gamma_n/(\pi\omega_B/8)$ varies exponentially with the ratio $(E_g/\hbar\omega_B)$; for $(E_g/\hbar\omega_B)\leq 0.1$, the tunneling rates for all models are within the same order of magnitude and slowly vary with E_g/ε_g; for $(E_g/\hbar\omega_B)\geq 0.3$, the exponential dependence on E_g/ε_g is significant in determining the value of γ_n. For small E_g/ε_g, the ENNTB and EMNNTB results coalesce, whereas the Kane result significantly departs from the ENNTB and the EMNNTB results in magnitude and slope due to the inappropriate application of the $\mathbf{k}\cdot\mathbf{P}$ perturbation theory in this band parameter regime; for E_g/ε_g increasing toward unity, the EMNNTB and Kane models coalesce, whereas the ENNTB result tends to the same limit at a different rate. In comparing the ENNTB and EMNNTB results, it is clear that when E_g/ε_g is small, the exact and effective-mass limits coalesce; the similarity in the two results in this limit is reflective of strong tunneling rates for the band gap near $K\sim 0$. On the other hand, as E_g/ε_g approaches unity for this comparison, the degree of nonparabolicity decreases in the nearest-neighbor tight-binding model, and the tunneling rate is high for many K values in the Brillouin zone due to a somewhat uniform band-gap; the difference in the ENNTB and EMNNTB results in this limit is reflective of the effective-mass limit favoring the dependence of band structure near $K\sim 0$, whereas the exact analysis reflects the global average in the K space of the energy-band difference.

Having illustrated the sensitivity analysis of the ENNTB, EMNNTB, and Kane models in Fig. 1, we now show in Fig. 2 the dependence of γ_n on $\hbar\omega_B$ specifically for bulk GaAs (Ref. 17) ($E_g\approx 1.5$ eV, $\varepsilon_g = E_g + W_1 + W_2 \approx 10$ eV, and $a\approx 5.6$ Å), and a GaAs/AlAs superlattice[18] ($E_g\approx 0.207$ eV, $\varepsilon_g = E_g + W_1 + W_2 \approx 0.252$ eV, and $a\approx 85$ Å). As observed, for both bulk and superlattice cases, the ENNTB

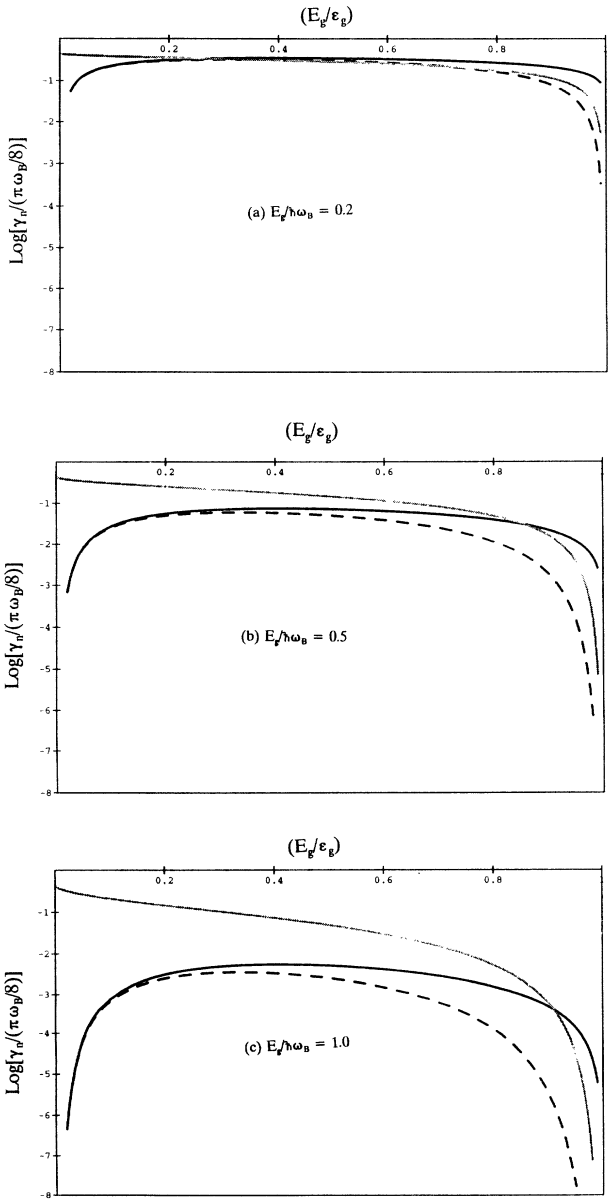

FIG. 1. Plot of $\log_{10}[\gamma_n/(\pi\omega_B/8)]$ of Eq. (79) vs (E_g/ε_g) comparing C_{ENNTB} (solid line), C_{EMNNTB} (dashed line), and C_{Kane} (gray solid line) defined by Eqs. (80), (83), and (85c); (a), (b), and (c) show relative variations of $E_g/\hbar\omega_B$.

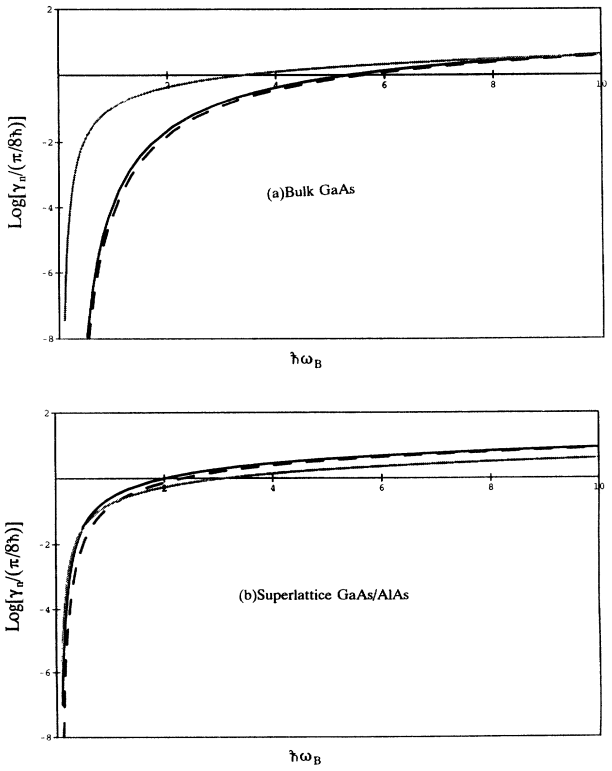

FIG. 2. Plot of $\log_{10}[\gamma_n/(\pi/8\hbar)]$ vs $(\hbar\omega_B)$ ($\hbar\omega_B$ in eV) comparing C_{ENNTB} (solid line), C_{EMNNTB} (dashed line), and C_{Kane} (gray solid line); (a) bulk GaAs ($E_g\approx 1.5$ eV, $\varepsilon_g\approx 10$ eV, and $a\approx 5.6$ Å), and (b) superlattice GaAs/AlAs ($E_g\approx 0.207$ eV, $\varepsilon_g\approx 0.252$ eV, and $a\approx 85$ Å).

and EMNNTB models are within the same order of magnitude, whereas the Kane model significantly differs relative to the ENNTB and EMNNTB results except for the bulk case in very high electric fields. It is interesting to note that, in general, $(E_g)_{\text{Bulk}} \sim 10(E_g)_{\text{SL}}$, $(E_g/\varepsilon_g)_{\text{Bulk}} \sim (1/10)(E_g/\varepsilon_g)_{\text{SL}}$, and therefore $[E_g \hbar\omega_B]_{\text{Bulk}} \approx 10(\hbar\omega_B)_{\text{SL}}[E_g/\hbar\omega_B]_{\text{SL}}/(\hbar\omega_B)_{\text{Bulk}}$ are order-of-magnitude scaling rules with regard to observing the variation in γ_n with each model in Fig. 1 for a range of bulk and superlattice band-structure parameters.

γ_n in Eqs. (79) and (80) derived from the ENNTB two-band model consideration is also estimated for some values of field; the explicit known band-parameter dependence therein serves to easily illustrate the sensitive dependence of γ_n on electric field. We note that when a field strength of $E_0 = 10^6$ V/cm is employed for GaAs (Ref. 17) ($a \approx 5.6$ Å, $E_g \approx 1.5$ eV, and $\varepsilon_g \approx 10$ eV), we obtain a Zener tunneling time $\tau_z \approx 10^{46}\tau_B$; $\tau_B = h/eE_0a \approx 0.74\times10^{-13}$ sec, and therefore $\tau_z \approx 2\times10^{25}$ years, so that the Zener tunneling time is so long that it can be ignored. However, when the field strength is increased by just one order of magnitude to $E_0 = 10^7$ V/cm, the Zener tunneling probability is increased significantly; here the Zener tunneling time $\tau_z \approx 3.7\times10^6\tau_B$, with $\tau_B = 0.74\times10^{-14}$ sec, and $\tau_z \approx 2.7\times10^{-8}$ sec, so that it still takes many Bloch oscillations to Zener tunnel out of the band, i.e., $\tau_z \gg \tau_B$, but with a relatively short Zener time. In noting that the Zener tunneling probability is very sensitive to the field strength and the band gap, appreciable Zener tunneling can be expected in superlattices, for which the band gap is 1–2 orders of magnitude smaller than a typical bulk crystalline solid, in moderately high field.

Finally, we examine the properties of the excited-state envelope functions in the Wigner-Weisskopf approximation. In this regard, since $A_n(\mathbf{K},t)$ has been found in Eq. (55), we can then determine $A_{n'}(\mathbf{K},t)$ from Eq. (37), and then $f_{n'}(l,t)$ from Eq. (12). Integrating Eq. (37), while using $A_n(\mathbf{K},0)$ of Eq. (55) on the right-hand side, we find that,

$$A_{n'}(\mathbf{K},t) = A_n(\mathbf{K},0)\left\{ i\frac{eE_0}{\hbar}\sum_{l_x} D^*_{nn'}(l_x,\mathbf{K}_\perp)e^{-iK_x a l_x}\frac{e^{i[-l_x\omega_B+\omega_{nn'}(\mathbf{K}_\perp)+\Delta\omega_n(\mathbf{K}_\perp)]t-[\gamma_n(\mathbf{K}_\perp)/2]t}-1}{i[-l_x\omega_B+\omega_{nn'}(\mathbf{K}_\perp)+\Delta\omega_n(\mathbf{K}_\perp)]-\gamma_n(\mathbf{K}_\perp)/2}\right\}, \tag{86}$$

where the summation over "l_x" reflects interactions with all possible lattice sites. It then follows from $f_{n'}(l,t)$, as given by using Eq. (86) in Eq. (12), that

$$f_{n'}(l,t) = i\frac{eE_0}{\hbar}\sum_{l'}\Delta^*_{nn'}(l')g_{n'}(l-l',t)\ , \tag{87}$$

where

$$g_{n'}(l-l',t) = \frac{1}{N}\sum_{\mathbf{K}} e^{-i/\hbar\int_0^t \epsilon_{n'}[\mathbf{K}-(e/\hbar c)\mathbf{A}_0]dt'} e^{i\mathbf{K}\cdot(l-l')}\omega(l_x,\mathbf{K}_\perp,t)A_n(\mathbf{K},0)\ , \tag{88}$$

and

$$\omega(l_x,\mathbf{K}_\perp,t) = \frac{e^{i[-l_x\omega_B+\omega_{nn'}(\mathbf{K}_\perp)+\Delta\omega_n(\mathbf{K}_\perp)]t-[\gamma_n(\mathbf{K}_\perp)/2]t}-1}{i[-l_x\omega_B+\omega_{nn'}(\mathbf{K}_\perp)+\Delta\omega_n(\mathbf{K}_\perp)]-\dfrac{\gamma_n(\mathbf{K}_\perp)}{2}}\ . \tag{89}$$

For an electron initially in band "n," with a mixed initial condition [Eq. (58)],

$$g_{n'}(l-l',s\tau_B) = \delta_{l'_x,l_x-l_{0x}}\frac{1}{\sqrt{N_\perp}}e^{-(i/\hbar)\bar{\epsilon}_{n'}(\mathbf{K}_{0\perp})s\tau_B}e^{i\mathbf{K}_{0\perp}\cdot(l-l')_\perp}\omega(l'_x,\mathbf{K}_{0\perp},s\tau_B)\ . \tag{90}$$

Therefore, after "s" Bloch period of time, the n'th band envelope function is

$$f_{n'}(l,s\tau_B) = i\frac{eE_0}{\hbar}D^*_{nn}(l_x-l_{0x},\mathbf{K}_{0\perp})\omega(l_x-l_{0x},\mathbf{K}_{0\perp},s\tau_B)\frac{1}{\sqrt{N_\perp}}e^{-(i/\hbar)\bar{\epsilon}_{n'}(\mathbf{K}_{0\perp})s\tau_B}e^{i\mathbf{K}_{0\perp}\cdot l_\perp}\ , \tag{91}$$

and the probability for an electron at band "n'" and site "l" is

$$|f_{n'}(l,s\tau_B)|^2 = \frac{1}{N_\perp}\left[\frac{eE_0}{\hbar}\right]^2|D_{nn'}(l_x-l_{0x},\mathbf{K}_{0\perp})|^2|\omega(l_x-l_{0x},\mathbf{K}_{0\perp},s\tau_B)|^2\ . \tag{92}$$

Then the total probability for an electron to be in band "n'" and located at sites with same position "l_x," a condition resembling the situation in a one-dimensional superlattice, is

$$\rho_{n'}(l_x,s\tau_B)\equiv\sum_{l'}|f_{n'}(l',s\tau_B)|^2\delta_{l'_x,l_x}$$
$$=\left[\frac{eE_0}{\hbar}\right]^2|D_{nn'}(l_x-l_{0x},\mathbf{K}_{0\perp})|^2|\omega(l_x-l_{0x},\mathbf{K}_{0\perp},s\tau_B)|^2$$
$$=\left[\frac{eE_0}{\hbar}\right]^2\frac{\{1+e^{-\gamma_n(\mathbf{K}_{0\perp})s\tau_B}-2e^{-[\gamma_n(\mathbf{K}_{0\perp})/2]s\tau_B}\cos[(\omega_{nn'}(\mathbf{K}_{0\perp})+\Delta\omega_n(\mathbf{K}_{0\perp}))s\tau_B]\}|D_{nn'}(l_x-l_{0x},\mathbf{K}_{0\perp})|^2}{[-(l_x-l_{0x})\omega_B+\omega_{nn'}(\mathbf{K}_{0\perp})+\Delta\omega_n(\mathbf{K}_{0\perp})]^2+\gamma_n^2(\mathbf{K}_{0\perp})/4}\ , \tag{93}$$

which is spatially broadened, even when the electron is initially localized in the direction of the electric field. It is noted that in the limit of $s\rightarrow\infty$, $\rho_{n'}(l_x,s\tau_B)$ reduces to

$$\rho_{n'}(l_x,\infty)=\left[\frac{eE_0}{\hbar}\right]^2\frac{|D_{nn'}(l_x-l_{0x},\mathbf{K}_{0\perp})|^2}{[-(l_x-l_{0x})\omega_B+\omega_{nn'}(\mathbf{K}_{0\perp})+\Delta\omega_n(\mathbf{K}_{0\perp})]^2+\gamma_n^2(\mathbf{K}_{0\perp})/4}$$
$$\equiv\frac{\omega_B^2}{16}\frac{e^{-2q_{nn'}(\mathbf{K}_{0\perp})a|l_x-l_{0x}|}}{[(l_x-l_{0x})\omega_B+\omega_{nn'}(\mathbf{K}_{0\perp})+\Delta\omega_n(\mathbf{K}_{0\perp})]^2+\gamma_n^2(\mathbf{K}_{0\perp})/4}\ . \tag{94}$$

V. DISCUSSION AND SUMMARY

A multiband theory of Bloch-electron dynamics in a homogeneous electric field of arbitrary strength has been presented. The analysis was developed in terms of Wannier envelope functions to accommodate the inherent localization manifest for Bloch dynamics in strong electric fields. The multiband coupling was treated using the Wigner-Weisskopf approximation; from this approximation, a generalized Zener tunneling time is derived in terms of explicit band-coupling parameters, and excited-state envelope functions were derived showing spatial delocalization and probability amplitude broadening as tunneling to the upper states occurs.

The combined use of the vector potential gauge, and therefore the concomitant use of time-dependent accelerated states, and the Wigner-Weisskopf approximation have allowed for the temporal analysis of Bloch-electron dynamics covering a time span from several Bloch oscillations to times well beyond the Zener tunneling time. In particular, a general three-dimensional time evolution kernel and envelope function was derived for single-band dynamics in electric fields of arbitrary strength. Use was made of familiar, analytic models in both one and three dimensions to illustrate and confirm the utility of the result. The general result can be incorporated into simulations and numerical modeling codes to include, in a user friendly way, the effects of the electric field with realistic band structures.

In using the Wigner-Weisskopf approximation in a multiband analysis, a general three-dimensional envelope function was derived which describes band dynamics including the effects of Zener tunneling, excited-state broadening due to the presence of the electric field, and dependence on the initial conditions. With regard to Zener tunneling times, a general three-dimensional expression for the Zener tunneling time was derived which shows the correct explicit dependence on quantum-mechanical initial conditions and the real band-structure parameters. Although the field dependence of the Zener tunneling time is identical to that of previous researches,[12,19] our result shows the importance of the average value of the band difference over the Brillouin zone rather than simply the gap itself. We demonstrate this important difference using the well-known nearest-neighbor tight binding model, and show the distinct difference in band parameter dependence compared with other well-known models.

In future work, we will be using the results to develop further the theory of Bloch-electron dynamics to include the effects of electric fields on scattering from defects, barriers, and phonons.

ACKNOWLEDGMENTS

This work was supported by Office of Naval Research and U.S. Army Research Office. The authors thank J. B. Krieger for critical comments and suggestions.

APPENDIX A: INTEGRATION OF THE TIME-DEPENDENT ENERGY-BAND FUNCTION

The integral of the time-dependent energy-band function

$$I_n=\int_0^t\epsilon_n\left[K-\frac{e}{\hbar c}A_0\right]dt' \tag{A1}$$

appears frequently as an exponent in the text of this paper. This existence of the electric field destroys the linear time dependence of the integral I_n. In this appendix, we study this integral for a general energy-band function $\epsilon_n(\mathbf{K})$ under the influence of a homogeneous electric field $\mathbf{E}_0$.

Since the energy-band function $\epsilon_n(\mathbf{K})$ can be expressed in a Fourier series expansion,

$$\epsilon_n(\mathbf{K})=\sum_l\varepsilon_n(l)e^{i\mathbf{K}\cdot l}\ , \tag{A2}$$

where $\varepsilon_n(l)$ are the Fourier transform of $\epsilon_n(\mathbf{K})$ with respect to the lattice site of the crystal potential, the time dependence of the energy-band function in (A1) is exhibited explicitly through the exponent of the Fourier series as

$$\epsilon_n\left[\mathbf{K}-\frac{e}{\hbar c}A_0\right]=\sum_l \varepsilon_n(l)e^{i\mathbf{K}\cdot l+i(e\mathbf{E}_0\cdot l)/(\hbar)t} . \quad \text{(A3)}$$

If the electric field is in the x direction, then Eq. (A3) becomes

$$\epsilon_n\left[\mathbf{K}-\frac{e}{\hbar c}A_0\right]=\sum_l \varepsilon_n(l)e^{i\mathbf{K}\cdot l+i\omega_B l_x t} , \quad \text{(A4)}$$

where l_x takes on the values $0,\pm1,\pm2,\ldots$.

Integrating Eq. (A4) term by term with time ranging from zero to "t," we obtain

$$I_n=\sum_{l,l_x=0}\varepsilon_n(l)e^{i\mathbf{K}\cdot l}t+\sum_{l,l_x\neq0}\varepsilon_n(l)e^{i\mathbf{K}\cdot l}\frac{e^{i\omega_B l_x t}-1}{i\omega_B l_x}$$

$$=\bar{\epsilon}_n(\mathbf{K}_\perp)t+\sum_{l_x\neq0}\varepsilon_n(l_x,\mathbf{K}_\perp)e^{iK_x a l_x}\frac{e^{i\omega_B l_x t}-1}{i\omega_B l_x} , \quad \text{(A5)}$$

where $\bar{\epsilon}_n(\mathbf{K}_\perp)$ is given by Eq. (20), the average value of energy-band function $\epsilon_n(\mathbf{K})$ along the K_x direction in the Brillouin zone, and

$$\varepsilon_n(l_x,\mathbf{K}_\perp)=\sum_{l_\perp}\varepsilon_n(l_x,l_\perp)e^{i\mathbf{K}_\perp\cdot l_\perp}$$

$$=\frac{1}{N_x}\sum_{K_x}\epsilon_n(K_x,\mathbf{K}_\perp)e^{-iK_x a l_x} . \quad \text{(A6)}$$

As "t" tends to become greater than $10\tau_B$, the phase factor $e^{i\omega_B l_x t}$ in Eq. (A5) becomes a rapidly oscillatory function of $\omega_B l_x$; thus, in treating the sum over $l_x\neq0$ in Eq. (A5) as a Poisson sum (Ref. 16; also see Appendix B), while noting that

$$\frac{e^{i\omega_B l_x t}-1}{\omega_B l_x}\approx -P\left[\frac{1}{\omega_B l_x}\right]+i\pi\delta(\omega_B l_x) \quad \text{(A7)}$$

for $t\geq 10\tau_B$, Eq. (A5) reduces to

$$I_n\approx\bar{\epsilon}_n(\mathbf{K}_\perp)t-\sum_{l_x\neq0}\frac{\varepsilon_n(l_x,K_\perp)}{i\omega_B l_x}e^{iK_x a l_x} . \quad \text{(A8)}$$

Thus the first term on the right-hand side of Eq. (A8) is linearly dependent on time, and the second term is independent of time; also the second term tends to be small in high electric field when I_n is evalauted as a phase term.

APPENDIX B: DERIVATION OF EQUATION (52)

A sum can always be equivalently represented by a series of Fourier integrals through the use of the "Poisson sum formula"[16]

$$\sum_{n=-\infty}^{\infty} f(n)\equiv\sum_{m=-\infty}^{\infty}\int_{-\infty}^{\infty} f(x)e^{i2\pi mx}dx . \quad \text{(B1)}$$

The identity in Eq. (B1) can be validated through a straightforward manipulation of the sum over $e^{i2\pi mx}$ by the use of

$$\sum_{m=-\infty}^{\infty} e^{iaxm}=\frac{2\pi}{a}\sum_{l=-\infty}^{\infty}\delta\left[x-\frac{2\pi}{a}l\right] . \quad \text{(B2)}$$

When the Poisson sum formula is applied to the sum in Eq. (52), the sum can be written as,

$$\lim_{\epsilon\to0}\sum_{l_x}\frac{|D_{nn'}(l_x,\mathbf{K}_\perp)|^2}{(-\omega_B l_x+\omega_{nn'}-i\epsilon)}$$

$$\equiv\sum_{m=-\infty}^{\infty}\lim_{\epsilon\to0}\int_{-\infty}^{\infty}\frac{|D_{nn'}(x,\mathbf{K}_\perp)|^2e^{i2\pi mx}}{(-\omega_B x+\omega_{nn'}-i\epsilon)}dx , \quad \text{(B3)}$$

where $\omega_{nn'}\equiv\omega_{nn'}(\mathbf{K}_\perp)$ as denoted in the text. Using $\lim_{\epsilon\to0}(1/x-i\epsilon)=P(1/x)+i\pi\delta(x)$ for the integrand of Eq. (B3) in the limit of $\epsilon\to0$, we can separate the right-hand side of Eq. (B3) into real part and imaginary parts as

$$\lim_{\epsilon\to0}\sum_{m=-\infty}^{\infty}\int_{-\infty}^{\infty}\frac{|D_{nn'}(x,\mathbf{K}_\perp)|^2e^{i2\pi mx}}{(-\omega_B x+\omega_{nn'}-i\epsilon)}dx$$

$$=P\int_{-\infty}^{\infty}dx\left[\frac{1}{\omega_{nn'}-\omega_B x}\right]|D_{nn'}(x,\mathbf{K}_\perp)|^2\sum_{m=-\infty}^{\infty}e^{i2\pi mx}+\frac{i\pi}{\omega_B}\left|D_{nn'}\left[\frac{\omega_{nn'}}{\omega_B},\mathbf{K}_\perp\right]\right|^2\sum_{m=-\infty}^{\infty}e^{i2\pi m(\omega_{nn'}/\omega_B)} . \quad \text{(B4)}$$

Using Eq. (B2) for the summations on the right-hand side of Eq. (B4), we obtain

$$\lim_{\epsilon\to0}\sum_{l_x}\frac{|D_{nn'}(l_x,\mathbf{K}_\perp)|^2}{(-\omega_B l_x+\omega_{nn'}-i\epsilon)}=\sum_{l_x}P\frac{|D_{nn'}(l_x,\mathbf{K}_\perp)|^2}{(\omega_{nn'}-\omega_B l_x)}+i\pi\left|D_{nn'}\left[\frac{\omega_{nn'}}{\omega_B},\mathbf{K}_\perp\right]\right|^2\sum_{l_x}\delta(\omega_{nn'}-\omega_B l_x) , \quad \text{(B5)}$$

which is essentially Eq. (52) after the sum over the band index is performed. Specially, $\Delta\omega_n$ and $\gamma_n/2$ in Eq. (52) become

$$\Delta\omega_n(\mathbf{K}_\perp)=\left[\frac{eE_0}{\hbar}\right]^2\sum_{n'\neq n}\sum_{l_x}P\frac{|D_{nn'}(l_x,\mathbf{K}_\perp)|^2}{(\omega_{nn'}-\omega_B l_x)} \tag{B6}$$

and

$$\begin{aligned}\frac{\gamma_n(\mathbf{K}_\perp)}{2}&=\pi\left[\frac{eE_0}{\hbar}\right]^2\sum_{n'\neq n}\left|D_{nn'}\left[\frac{\omega_{nn'}}{\omega_B},\mathbf{K}_\perp\right]\right|^2\\&\quad\times\sum_{l_x}\delta(\omega_{nn'}-l_x\omega_B)\\&=\frac{\pi}{\omega_B}\left[\frac{eE_0}{\hbar}\right]^2\sum_{n'\neq n}\left|D_{nn'}\left[\frac{\omega_{nn'}}{\omega_B},\mathbf{K}_\perp\right]\right|^2,\end{aligned} \tag{B7}$$

In Eq. (B7), it is noted that the density of states for a Bloch electron implicitly includes the Stark-ladder spectrum in the electric field, so that

$$\begin{aligned}\sum_{l_x}\delta(\omega_{nn'}-l_x\omega_B)&=\hbar\sum_{l_x}\delta[\bar{\epsilon}_{n'}(\mathbf{K}_\perp)-\bar{\epsilon}_n(\mathbf{K}_\perp)-l_x\hbar\omega_B]\\&=\hbar\rho(\epsilon)\ ,\end{aligned} \tag{B8}$$

where $\rho(\epsilon)$ is the density of the states given by $(1/\hbar\omega_B)$.[20,21]

APPENDIX C: CALCULATION OF $D_{nn'}(l_x,\mathbf{K}_\perp)$

Since $\gamma_n(\mathbf{K}_\perp)$, the exponential decay rate of $A_n(\mathbf{K},t)$, is dictated by the value of $D_{nn'}(l_x,\mathbf{K}_\perp)$ at $l_x\approx l_{nn'}(\mathbf{K}_\perp)$ as indicated in Eq. (54), it is necessary to calculate $D_{nn'}(l_x,\mathbf{K}_\perp)$ for given bands of $\epsilon_n(\mathbf{K})$ and $\epsilon_{n'}(\mathbf{K})$. $D_{nn'}(l_x,\mathbf{K}_\perp)$ is defined in the text as

$$\begin{aligned}D_{nn'}(l_x,\mathbf{K}_\perp)&=\sum_{\boldsymbol{l}_\perp}\Delta_{nn'}(\boldsymbol{l})e^{i\mathbf{K}_\perp\cdot\boldsymbol{l}_\perp}\\&=\frac{1}{N_x}\sum_{\mathbf{K}_x}X_{nn'}(\mathbf{K})e^{-iK_x a l_x}\ ,\end{aligned} \tag{C1}$$

where $X_{nn'}(\mathbf{K})$ is the x component of the interband coupling parameter $\mathbf{R}_{nn'}(\mathbf{K})$,

$$\mathbf{R}_{nn'}(\mathbf{K})=\frac{i}{\Omega}\int dx\ U^*_{n\mathbf{K}}\nabla_{\mathbf{K}}U_{n'\mathbf{K}}\ . \tag{C2}$$

The summation in Eq. (C1) can be converted into an integral over K_x from 0 to $2\pi/a$ as

$$D_{nn'}(l_x,\mathbf{K}_\perp)=\frac{a}{2\pi}\int_0^{2\pi/a}X_{nn'}(\mathbf{K})e^{-iK_x a l_x}dK_x\ . \tag{C3}$$

Krieger has shown[22] that near the connection point of bands "n" and "n',"

$$X_{nn'}(K_x,\mathbf{K}_\perp)|_{K_x\sim q}\approx\pm\frac{1}{4(K_x-q)}\ , \tag{C4}$$

where the connection point of the bands, "q," is determined by $\epsilon_n(q,K_\perp)=\epsilon_{n'}(q,K_\perp)$. The connection point is, in fact, the pole of the integrand in Eq. (C3) with residue $\pm 2\pi i/4$ for $X_{nn'}(K_x,K_\perp)$ at $K_x=q$. The integral of Eq. (C3) can be converted to a complex contour integral and be evaluated by residue theorem to give

$$D_{nn'}(l_x,\mathbf{K}_\perp)=\pm i\frac{a}{4}e^{-iqal_x}\ . \tag{C5}$$

For a fixed $\mathbf{K}_\perp$, the value of "q" depends on specific band functions of $\epsilon_n(\mathbf{K})$ and $\epsilon_{n'}(\mathbf{K})$, where "$q$" is generally a purely imaginary number. For $q=\pm iq_{nn'}(\mathbf{K}_\perp)$, it follows that

$$D_{nn'}(l_x,\mathbf{K}_\perp)=\pm\frac{i}{4}ae^{-|q_{nn'}(\mathbf{K}_\perp)al_x|}\ . \tag{C6}$$

[1] J. B. Krieger and G. J. Iafrate, Phys. Rev. B **33**, 5494 (1986).
[2] J. B. Krieger and G. J. Iafrate, Phys. Rev. B **35**, 9644 (1987).
[3] G. J. Iafrate and J. B. Krieger, Phys. Rev. B **40**, 6144 (1989).
[4] H. G. Roskos, M. C. Nuss, J. Shah, K. Leo, D. A. B. Miller, A. M. Fox, S. Schmitt-Rink, and K. Köhler, Phys. Rev. Lett. **68**, 2216 (1992).
[5] C. Waschke, H. G. Roskos, R. Schwedler, K. Leo, H. Kurz, and K. Köhler, Phys. Rev. Lett. **70**, 3319 (1993).
[6] J. Feldmann, K. Leo, J. Shah, D. A. B. Miller, J. E. Cunningham, T. Meier, G. Von Plessen, A. Schulze, P. Thomas, and S. Schmitt-Rink, Phys. Rev. B **46**, 7252 (1992).
[7] A. Sibille, J. F. Palmier, H. Wang, and F. Mollot, Phys. Rev. Lett. **64**, 52 (1990).
[8] A. Sibille, J. F. Palmier, and F. Mollot, Appl. Phys. Lett. **60**, 457 (1992).
[9] A. Sibille, J. F. Palmier, H. Wang, J. C. Esnault, and F. Mollot, Appl. Phys. Lett. **56**, 256 (1990).
[10] P. England, J. R. Hayes, E. Colas, and H. Helm, Phys. Rev. Lett. **63**, 1708 (1989).
[11] E. Merzbacher, *Quantum Mechanics* (Wiley, New York, 1970).
[12] E. O. Kane, J. Phys. Chem. Solids **12**, 181 (1959).
[13] P. T. Landsberg, *Solid State Theory Methods and Applications* (Wiley-Interscience, New York, 1969).
[14] M. Abramowitz and I. A. Stegun, *Handbook of Mathematical Functions* (Dover, New York, 1972).
[15] M. L. Goldberger and K. M. Watson, *Collision Theory* (Wiley, New York, 1964).
[16] P. M. Morse and H. Feshbach, *Methods of Theoretical Physics* (McGraw-Hill, New York, 1953).
[17] D. N. Talwan and C. S. Ting, Phys. Rev. B **25**, 2660 (1982).
[18] L. Esaki and L. L. Chang, Phys. Rev. Lett. **33**, 495 (1974).
[19] L. V. Keldysh, Pis'ma Zh. Eksp. Teor. Fiz. **33**, 994 (1957) [JETP Lett. **6**, 763 (1958)].
[20] P. J. Price, in *Handbook on Semiconductors,* edited by P. T. Landsberg (North-Holland, New York, 1992), Vol. 1, Chap. 12.
[21] J. Callaway, *Quantum Theory of the Solid State,* 2nd ed. (Academic, New York, 1991).
[22] J. B. Krieger, Phys. Rev. **156**, 776 (1967).